Weierstraß-Institut
für Angewandte Analysis und Stochastik

im Forschungsverbund Berlin e.V.

Preprint ISSN 0946 – 8633

Ultrafast spatio-temporal dynamics of terahertz generation by ionizing two-color femtosecond pulses in gases

Ihar Babushkin[1], Wilhelm Kuehn[2], Christian Köhler[3], Stefan Skupin[3,4], Luc Bergé[5], Klaus Reimann[2], Michael Woerner[2], Joachim Herrmann[2], and Thomas Elsaesser[2]

submitted: 10 Mar. 2010

[1] Weierstrass Institute for Applied Analysis and Stochastics Mohrenstr. 39 10117 Berlin Germany, E-mail: babushkin@wias-berlin.de

[2] Max Born Institute for Nonlinear Optics and Short Time Spectroscopy, Max-Born-Str. 2A, 12489, Berlin, Germany.

[3] Max Planck Institute for the Physics of Complex Systems Nöthnitzer Str. 38 01187 Dresden Germany

[4] Friedrich Schiller University Institute of Condensed Matter Theory and Optics Fröbelstieg 1 07742 Jena Germany

[5] CEA-DAM, DIF, F-91297 Arpajon, France

No. 1488

Berlin 2010

2000 *Mathematics Subject Classification.* 78A60, 35Q61, 35Q60.

Key words and phrases. THz light generation, Photoionization, Ultrashort pulse propagation.

1999 *Physics and Astronomy Classification Scheme.* 42.65.Re, 32.80.Fb, 52.50.Jm, 42.65.-k.

Edited by
Weierstraß-Institut für Angewandte Analysis und Stochastik (WIAS)
Mohrenstraße 39
10117 Berlin
Germany

Fax: + 49 30 2044975
E-Mail: preprint@wias-berlin.de
World Wide Web: http://www.wias-berlin.de/

Abstract

We present a combined theoretical and experimental study of spatio-temporal propagation effects in terahertz (THz) generation in gases using two-color ionizing laser pulses. The observed strong broadening of the THz spectra with increasing gas pressure reveals the prominent role of spatio-temporal reshaping and of a plasma-induced blue-shift of the pump pulses in the generation process. Results obtained from (3+1)-dimensional simulations are in good agreement with experimental findings and clarify the mechanisms responsible for THz emission.

Far-infrared radiation in the THz range has developed into a sensitive probe of low-frequency excitations of condensed matter and into an analytical and imaging tool for a broad range of applications. Recently, intense THz pulses have been applied for inducing nonlinear light-matter interactions and for studying quantum-coherent charge transport phenomena in solids. In this new area of research, the generation of well-defined THz field transients with a high amplitude represents a key issue. Both electron accelerator- and laser-based sources have been developed to generate THz transients. Conventional laser-driven THz sources are based on semiconductor photoconductive switches [1] and nonlinear frequency conversion in crystals [2], providing a comparably small THz field strength in a spectral range limited by the absorption of the crystals. In an alternative approach [3], a short pump pulse at 800 nm and its second harmonic at 400 nm are focused into a gaseous medium to generate a plasma. Intense THz pulses with field amplitudes as high as 400 kV/cm and remarkably broad spectra have been reported with this method [3–13]. However, the physical mechanisms behind the observed THz generation remain controversial. Initially, THz generation has been explained by four-wave mixing rectification [3, 14] and experimental results have been interpreted along those lines (see, e.g., [4–6, 8, 13]). In contrast, other studies attribute THz emission to a laser-induced plasma current in the asymmetric two-color laser field [9, 10, 12]. So far, theoretical work has mainly focused on the analysis of local fields by using photocurrent models. An alternative approach is based on particle in cell simulations [15–17] which are computationally very expensive and limited to propagation lengths of a few micrometers only.

In this Letter we present a combined theoretical and experimental study of THz generation by ionizing two-color femtosecond pulses in a gas. Extensive numerical simulations were performed using for the first time a (3+1)-dimensional code based on an unidirectional pulse propagation equation which includes the plasma dynamics responsible for the observed THz generation. This approach allows a comprehensive description of the propagation of all fields taking into account their spatio-temporal reshaping induced by the plasma effects and the optical Kerr nonlinearity. We demonstrate that spatio-temporal propagation effects are indispensable for understanding the generation process and influence the THz spectrum substantially. In both experiments and simulations we observe a remarkable broadening of the THz spectrum with increasing gas pressure. Such broadening is a result of a sensitive dependence of the THz spectrum on small phase and frequency shifts induced by nonlinear propagation of the fundamental and second harmonic pulses.

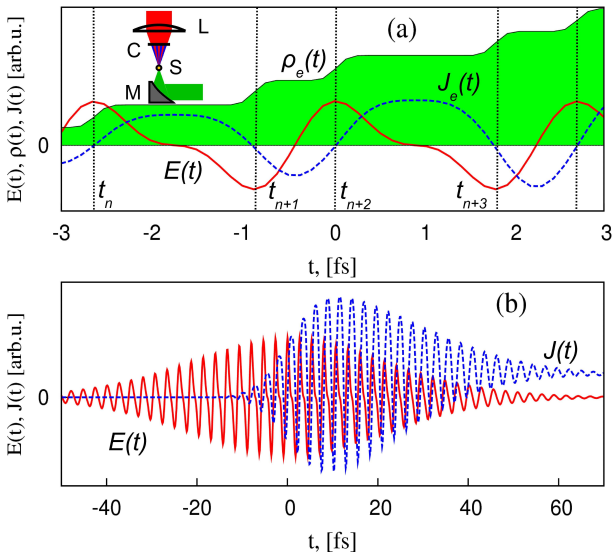

Figure 1: (color online) The mechanism of THz generation: (a) The two-color electric field E generates free electrons with a step-wise modulation of the electron density ρ via tunneling photoionization. The ionization occurs mostly near the maxima of electric field at time instances t_n. (b) This leads to a slow component of the current J growing on time scales of the pulse duration, which acts as a source for THz emission. Inset in (a): scheme of the experimental setup.

We show that the stepwise character of the ionization process on the sub-femtosecond time scale is essential for such dependence.

Our THz plasma source (inset of Fig. 1) is driven by 40 fs pulses (800 nm) with pulse energies of $\sim$ 300 μJ at a repetition rate of 1 kHz from a Ti:sapphire laser system. Intensities far above the field ionization threshold are reached by focusing the beam of 8 mm diameter with an achromatic lens (L) of 40 mm focal length. A 0.1 mm thin β-barium borate (BBO) crystal (C) cut for type I second-harmonic generation is additionally inserted into the convergent beam 7 mm before the focus. The setup is placed in a closed chamber filled with argon at various pressures between 1 and 1000 mbar. THz radiation emitted from the plasma volume in the focal spot is collected by a parabolic mirror (M) with a diameter of 25.4 mm at a distance of its effective focal length of 12.7 mm. The THz spectrum is measured by a Michelson interferometer. Intensity interferograms were recorded with a mercury cadmium telluride (HgCdTe) detector by varying the path difference between the two arms, and the THz spectra were obtained by Fourier transformation.

For the description of the nonlinear propagation of electromagnetic fields valid in the full range from THz down to UV/VUV wavelengths beyond paraxial and slowly-varying envelope approximations we use the following unidirectional pulse propagation equation [21] for linearly polarized pulses

$$\partial_z \hat{E} = i\sqrt{k(\omega)^2 - k_x^2 - k_y^2}\,\hat{E} + i\frac{\mu_0\omega^2}{2k(\omega)}\hat{\mathcal{P}}_{\mathrm{NL}}. \tag{1}$$

Here, $\hat{E}(k_x, k_y, z, \omega)$ is the Fourier transform (indicated by $\hat{}$) of the electric field with respect to x, y, and t, $k(\omega) = \omega n(\omega)/c$ is the wavenumber, ω the frequency, c is the speed of light and $n(\omega)$ is the refractive index of the gaseous medium, in our case argon [19]. The

first term on the r.h.s. of Eq. (1) describes linear dispersion and diffraction of the pulse. The nonlinear polarization $\hat{\mathcal{P}}_{\rm NL} = \hat{P}_{\rm Kerr} + i\hat{J}_e/\omega + i\hat{J}_{\rm loss}/\omega$ originates from the optical Kerr effect $P_{\rm Kerr}$, the electron current J_e and a loss term $J_{\rm loss}$ due to photon absorption during ionization. In $\hat{P}_{\rm Kerr}$ we take into account different nonlinear susceptibilities for neutral atoms and ions [20]. However, the Kerr response has negligible influence on the THz spectrum. The plasma dynamics is described by the electron density $\rho_e(t)$, obeying

$$\dot{\rho}_e(t) = W_{\rm ST}(E)[\rho_{at} - \rho_e(t)], \tag{2}$$

where ρ_{at} denotes the neutral atomic density and dot the time-derivative. We use the quasi-static tunneling ionization rate for hydrogen-like atoms given by [10] $W_{\rm ST}(E) = 4\omega_a(r_H)^{2.5}[E_a/|E|]\exp[-2(r_H)^{1.5}E_a/3|E|]$, where $E_a = m_e^2q^5/\hbar^5, \omega_a = m_eq^4/\hbar^3$ and $r_H = U_h/U_{Ar}$. U_h and U_{Ar} are the ionization potentials of hydrogen and argon; m_e and q are the electron mass and charge, respectively. For the anticipated electric field strengths, we neglect multi-photon and avalanche ionization. The transverse macroscopic plasma current $J_e(t)$ is determined by the microscopic velocity distribution $v(t, t_0)$ of electrons born at the time t_0 [9, 10, 12],

$$J_e(t) = q\int_{-\infty}^{t} v(t, t_0)\dot{\rho}_e(t_0)dt_0. \tag{3}$$

Assuming zero velocity for new-born electrons and neglecting the influence of the magnetic field and electron-electron interaction, the electron velocity reads

$$v(t, t_0) = \frac{q}{m_e}\int_{t_0}^{t} E(\tau)\exp[-\nu_e(t-\tau)]d\tau, \tag{4}$$

where ν_e is the electron-ion collision rate. Substituting this into Eq. (3) we obtain

$$\dot{J}_e(t) + \nu_e J_e(t) = \frac{q^2}{m_e}E(t)\rho_e(t). \tag{5}$$

The above analysis demonstrates that we regain a well-known equation for the current (see, e.g., [20]). To formally ensure energy conservation during ionization, the additional term $J_{\rm loss} = W_{\rm ST}[E](\rho_{\rm at} - \rho_e)U_{Ar}/E$ is introduced in Eq. (1) such that the energy dissipation $J_{\rm loss}E$ equals the ionization energy loss.

Let us now illustrate the mechanism behind THz generation. In Fig. 1(a) we present the electron density (in green), which shows a stepwise increase near the tunnel ionization events at the field maxima (red curve). Such behavior has been recently observed in real-time experiments with sub-femtosecond resolution [18]. In a simplified model, we can assume rectangular steps in the electron density $[\dot{\rho}_e(t) = \Sigma_n\rho_n\delta(t - t_n)]$ and $\nu_e = 0$, and thereby obtain a discrete version of Eq. (3):

$$J_e(t) \sim \sum_n \rho_n H(t - t_n)[v_f(t) - v_f(t_n)], \tag{6}$$

where $H(t)$ is the Heaviside step function, $v_f(t) = \frac{q}{m_e}\int_{-\infty}^{t} E(\tau)d\tau$ is the free electron velocity such that $v(t, t_n) = [v_f(t) - v_f(t_n)]$, and ρ_n is the electron density created in the nth ionization event. For a monochromatic electric field $v_f(t_n) = 0$. The Fourier transformation of the step function $H(t)$ exhibits a low-frequency spectrum $\sim 1/\omega$, therefore

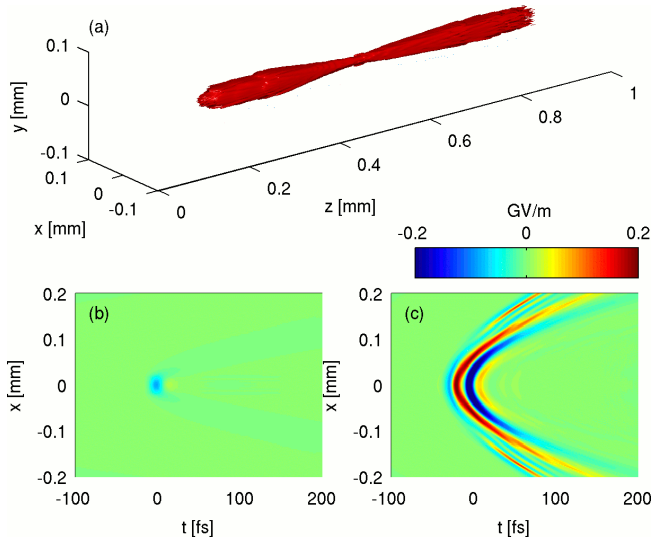

Figure 2: (color online) (a) Iso-electron-density surface at $\rho_e = 5 \times 10^{17}$ cm^{-3} for 200 mbar gas pressure. Computed THz fields ($\omega < 500$ ps^{-1}) at (b) $z = 0.2$ mm and (c) $z = 1$ mm.

THz radiation is generated by the terms in Eq. (6) proportional to $v_f(t_n)$, while the terms proportional to $v_f(t)$ contribute in the spectral range of the pump fields.

In order to model the experimental conditions in the plasma spot, we consider a Gaussian input beam with a waist $w_0 = 100$ μm and a duration of the 800 nm pump pulse of (FWHM) $t_p = 40$ fs (pulse energy 300 μJ). The energy of the second harmonic at 400 nm is chosen as 12% of the fundamental as estimated from the experiment. The duration t_p and the waist w_0 of the second harmonic are by a factor $\sqrt{2}$ smaller than the values for the fundamental. The phase angle between the two components is zero initially and shifts during propagation to non-zero values. The pulsed input beams are focused ($f = 0.5$ mm, in order to have a comparable ratio w_0/f in experiment and simulation) into the argon atmosphere. Figure 2 shows (a) the evolution of the computed plasma density and the transverse distribution of the THz field at (b) 0.2 mm and (c) 1 mm for a gas pressure of 200 mbar. The field intensities reach the ionization threshold shortly after the starting point of the simulation at $z = 0$ mm, and form a 0.7 mm long plasma channel. THz fields inside this focal region reach values of the order of GV/m and exhibit a strong diffraction.

Let us now investigate the dependency of THz generation on the gas pressure. Measured spectra over the complete pressure range between 1 mbar and 1000 mbar are shown as a contour plot in Fig. 3(a). Our HgCdTe detector is sensitive in a frequency range $\omega = 2\pi\nu$ from 125 ps^{-1} to 1070 ps^{-1}, i.e., the drop of the measured energy spectral density around 125 ps^{-1} is due to the decreasing sensitivity. For a comparison of theory and experiment, the high-frequency part of the spectra is most relevant. In our setup, we mainly detect THz radiation generated in the focus of the mirror (M). Simple ray tracing estimates indicate that the length of this focal region is $\lesssim 0.3$ mm. The almost vanishing spectrum at small argon pressure shows clearly that the plasma and not the BBO crystal acts as a source of the emitted radiation. In the region from zero to ~ 300 mbar the spectral width increases strongly. The highest frequencies even beyond 300 ps^{-1} are detected at pressures larger than 300 mbar. Above ~ 500 mbar the slope of the high frequency wing stays rather constant. The measured THz yield [solid line in Fig. 3(d)] grows linearly with the pressure up to 400 mbar before it saturates.

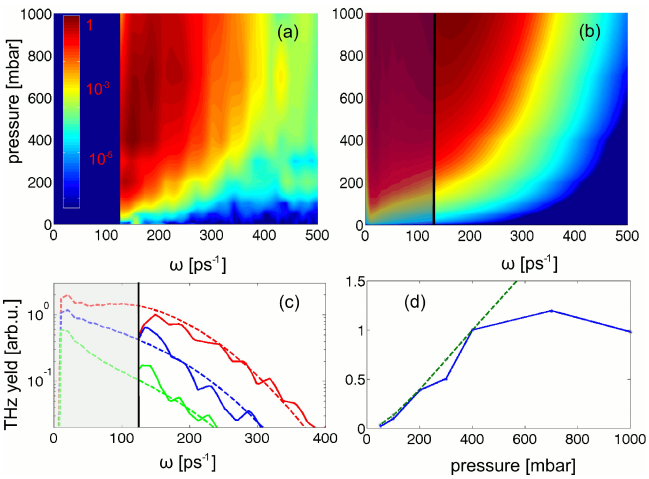

Figure 3: (color online). Measured THz spectra (a) and simulation results (b) for pressures between 1 and 1000 mbar. In (c), experimental (solid lines) and theoretical (dashed lines) spectra are compared for 100, 200 and 400 mbar (green, blue and red curves, resp.). In (b),(c), the part below $\omega = 125$ ps^{-1} is shaded, because no experimental values are available. In (d), the overall THz yield versus pressure is shown (dashed green line represents the simulation, solid line the experiment).

In Fig. 3(b,c), THz spectra computed with our simulation code are shown. The simulated spectra in Fig. 3(b,c) are obtained by integration over the transverse coordinates (x, y). We find very good agreement between experiment and simulation below 500 mbar for THz fields generated at the beginning of the plasma spot around $z = 0.2$ mm (0.3 mm before the linear focus). THz fields generated upon further propagation become spectrally much broader. Hence, we conjecture that the parabolic mirror in the experiment images the leading part of the plasma spot only. The calculated THz yield increases linearly with gas pressure [dashed line in Fig. 3(d)], in agreement with experimental results up to 400 mbar. The saturation of the experimental yield at higher pressure is likely due to additional THz losses upon further propagation towards the mirror, whereas the simulated yield is computed directly at the position $z = 0.2$ mm.

The observed pressure dependence of the THz spectral maximum and width gives insight into important features of plasma-induced THz generation. The dependence of the spectral width on pressure can not be explained by the local plasma current in which the variation of pressure results only into an amplitude scaling of the current. Instead, it originates from pressure dependent nonlinear propagation effects. For the intensity range and plasma interaction length of the experiment, the calculated spectral evolution of the pump pulses at 400 nm ($\omega = 2\pi \times 750$ THz) and 800 nm ($\omega = 2\pi \times 375$ THz) shows that their spectral broadening is negligible. We observe, however, small blue-shifts $\delta\omega$ of the central frequencies caused by the nonlinear plasma-induced change of the refraction index [22,23]. These shifts are ~ 6 ps^{-1} in the fundamental and ~ 2.5 ps^{-1} in the second harmonic at $z = 0.2$ mm for 400 mbar, and depend strongly on the gas pressure.

Surprisingly, these very small frequency shifts have a dramatic influence on the generated THz spectrum. This effect is most pronounced in the on-axis spectra, where the intensity is maximal. In Fig. 4(a), the calculated on-axis THz spectra are plotted for 400 mbar gas pressure, displaying dramatic changes in spectral shape and the maximum frequency between 0.1 mm (red curve) and 0.2 mm (blue curve). Figs. 4 (b,c) show the corresponding

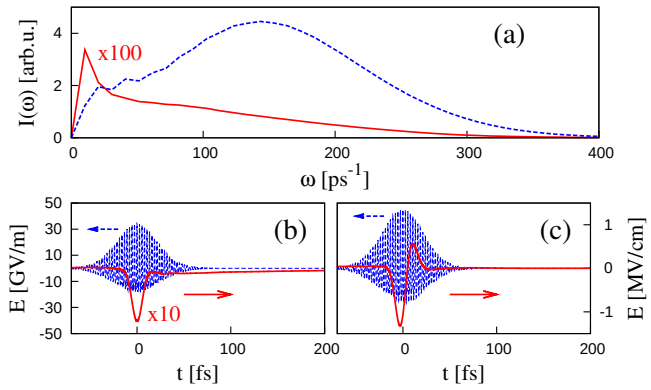

Figure 4: (color online) (a) On-axis ($x = 0, y = 0$) spectral intensity $I(\omega)$ and (b,c) temporal shape of $E(t)$ for 400 mbar gas pressure. In (a), $I(\omega)$ at $z = 0.1$ mm and $z = 0.2$ mm are shown by the solid red and dashed blue line, respectively. The temporal profiles of the field $E(t)$ (blue curve) and its low frequency part (red curve) are shown in (b) for $z = 0.1$ mm and in (c) for $z = 0.2$ mm. $I(\omega)$ and $E(t)$ at $z = 0.1$ mm [red curves in (a) and (b)] are amplified by a factor 100 and 10, respectively, in order to improve visibility.

time-dependent field and its low-frequency part. To explain the physical origin of this very sensitive dependence, let us go back to our simplified model [Eq. (6)]. For a two-color optical field, $E = A_1 \cos[(\omega_0 + \delta\omega)t] + A_2 \cos(2\omega_0 t + \theta)$, the field maxima in every half-cycle are given by $\omega_0 t_n \approx n\pi - n\pi\delta\omega/\omega_0 - (-1)^n 2r \sin\theta$, provided that $A_2/A_1 = r \ll 1$ and $n\delta\omega \ll \omega_0$. Hence, the points in time t_n and therefore the free velocities $v_f(t_n)$ alter significantly when $\delta\omega$ (and θ) change upon the propagation. As seen above, the low-frequency spectrum is determined by a sum over contributions $\sim v_f(t_n)$, and this sum finally determines the THz spectral shape in Fig. 4(a). In the full (3+1)-dimensional geometry, the spectral shapes generated at different spatial points are added and averaged, leading to the strong spectral broadening observed in Fig. 3(c). Thus, the above described dependence of the THz spectral shapes on pressure and propagation distance can be explained by propagation effects of the pump fields. We would like to stress that phase and frequency relation of fundamental and second harmonic fields always change during propagation.

In conclusion, we presented a theoretical and experimental investigation of photo-current induced THz generation. Using (3+1)-dimensional simulations and experimental measurements we show a strong dependence of the THz spectra on gas pressure. Our results give insight into the important influence of nonlinear propagation effects and the mechanism of THz generation. Plasma-induced blue-shifts of the driving pulses play a key role in the pressure dependent broadening of the THz spectra and confirm that the emission process of THz radiation is associated with a stepwise modulation of the tunneling ionization current. We believe that our findings open interesting perspectives to control THz emission in a broader spectral range.

This work has been performed using HPC resources from GENCI-CINES (Grant 2009-x2009106003).

References

[1] D. You, R. R. Jones, P. H. Bucksbaum, and D. R. Dykaar, Opt. Lett. **18**, 290 (1993).

[2] D. H. Auston, K. P. Cheung, J. A. Valdmanis, and D. A. Kleinman, Phys. Rev. Lett. **53**, 1555 (1984).

[3] D. J. Cook and R. M. Hochstrasser Opt. Lett. **25**, 1210 (2000).

[4] P. Zhang et al., Phys. Rev. Lett. **91**, 225001 (2003).

[5] M. Kress et al. Opt. Lett. **29**, 1120 (2004).

[6] T. Bartel et al., Opt. Lett. **30**, 2805 (2005).

[7] M. Kress et al., Nat. Phys. **2**, 327 (2006).

[8] Xu Xie, J. Dai, and X.-C. Zhang, Phys. Rev. Lett. **96**, 075005 (2006).

[9] K. Kim, J. Glownia, A. Taylor, and G. Rodriguez, Opt. Expr. **15**, 4577 (2007).

[10] M. D. Thomson, M. Kress, T. Loeffler, H. G. Roskos, Laser & Photon. Rev. **1**, 349 (2007).

[11] K. Reimann, Rep. Progr. Phys. **70**, 1597 (2007).

[12] K. Kim, J. Glownia, A. Taylor, and G. Rodriguez, Nat. Phot., **2**, 605 (2008).

[13] A. Houard, Yi Liu, B. Prade and A. Mysyrowicz, Opt. Lett. **33**, 1195 (2008).

[14] J. Peñano et al., Phys. Rev. E **81** 026407 (2010).

[15] H.-Ch. Wu, J. Meyer-ter-Vehn, and Zh.-M. Sheng, New J. Phys. **10**, 043001 (2008).

[16] M. Chen, A. Pukhov, X.-Yu Peng, and O. Willi, Phys. Rev. E **78**, 046406 (2008).

[17] W.-M. Wang et al., Opt. Expr. **16**, 16999 (2008).

[18] M. Uiberacker et al., Nature **446**, 627 (2007) .

[19] A. Dalgarno and A. E. Kingston, Proc. Royal Soc. London A **259**, 424 (1960).

[20] P. Sprangle, J. R. Penano, B. Hafizi, and C. A. Kapetanakos, Phys. Rev. E **69**, 066415 (2004).

[21] M. Kolesik and J. V. Moloney, Phys. Rev. E **70**, 036604 (2004).

[22] Wm. M. Wood, C. W. Siders, and M. C. Downer, Phys. Rev. Lett. 67, 3523 (1991).

[23] S.C. Rae and K. Burnett, Phys. Rev. A 46, 1084 (1992).